

Five enzymes of the Arg/N-degron pathway form a targeting complex: The concept of superchanneling

Jang-Hyun Oh^a, Ju-Yeon Hyun^a, Shun-Jia Chen^a, and Alexander Varshavsky^{a,1}

^aDivision of Biology and Biological Engineering, California Institute of Technology, Pasadena, CA 91125

Contributed by Alexander Varshavsky, February 28, 2020 (sent for review February 18, 2020; reviewed by Thomas Arnesen and William P. Tansey)

The Arg/N-degron pathway targets proteins for degradation by recognizing their N-terminal (Nt) residues. If a substrate bears, for example, Nt-Asn, its targeting involves deamidation of Nt-Asn, arginylation of resulting Nt-Asp, binding of resulting (conjugated) Nt-Arg to the UBR1-RAD6 E3-E2 ubiquitin ligase, ligase-mediated synthesis of a substrate-linked polyubiquitin chain, its capture by the proteasome, and substrate's degradation. We discovered that the human Nt-Asn-specific Nt-amidase NTAN1, Nt-Gln-specific Nt-amidase NTAQ1, arginyltransferase ATE1, and the ubiquitin ligase UBR1-UBE2A/B (or UBR2-UBE2A/B) form a complex in which NTAN1 Nt-amidase binds to NTAQ1, ATE1, and UBR1/UBR2. In addition, NTAQ1 Nt-amidase and ATE1 arginyltransferase also bind to UBR1/UBR2. In the yeast *Saccharomyces cerevisiae*, the Nt-amidase, arginyltransferase, and the double-E3 ubiquitin ligase UBR1-RAD6/UFD4-UBC4/5 are shown to form an analogous targeting complex. These complexes may enable substrate channeling, in which a substrate bearing, for example, Nt-Asn, would be captured by a complex-bound Nt-amidase, followed by sequential Nt modifications of the substrate and its polyubiquitylation at an internal Lys residue without substrate's dissociation into the bulk solution. At least in yeast, the UBR1/UFD4 ubiquitin ligase interacts with the 26S proteasome, suggesting an even larger Arg/N-degron-targeting complex that contains the proteasome as well. In addition, specific features of protein-sized Arg/N-degron substrates, including their partly sequential and partly nonsequential enzymatic modifications, led us to a verifiable concept termed "superchanneling." In superchanneling, the synthesis of a substrate-linked poly-Ub chain can occur not only after a substrate's sequential Nt modifications, but also before them, through a skipping of either some or all of these modifications within a targeting complex.

degron | channeling | superchanneling | ubiquitin | degradation

Regulated protein degradation protects cells from abnormal (e.g., misfolded or aggregated) proteins, and also mediates the levels of proteins that evolved to be constitutively or conditionally short-lived in vivo. The ubiquitin (Ub)-proteasome system (UPS) and the autophagy-lysosome system comprise two major sets of intracellular proteolytic pathways. Chaperone proteins are a part of both systems (1–10). Ub ligases of the UPS recognize substrate proteins through their degradation signals (degrons) and conjugate the 9-kDa Ub (usually a poly-Ub chain) to cognate amino acid residues (usually specific internal lysines) of targeted substrates. Deubiquitylases, another major class of UPS enzymes, catalyze deubiquitylation of Ub-conjugated proteins (2–4, 9–13). A substrate-linked poly-Ub chain is recognized by the ATP-dependent protease called the 26S proteasome. This protease unfolds the captured protein and processively converts it to ~10-residue peptides (14–19).

Several proteolytic systems, called N-degron pathways (previously called "N-end rule pathways"), have in common their ability to recognize proteins that contain N-terminal (Nt) degrons called N-degrons. This recognition causes degradation of targeted proteins by the 26S proteasome and autophagy in eukaryotes, and by the proteasome-like ClpAP protease in bacteria (Fig. 1 and *SI Appendix, Fig. S1*) (2, 9, 10, 20–48). An

N-degron comprises, in particular, a destabilizing Nt-residue of a protein and its internal Lys residue(s) that acts as a site of polyubiquitylation (2, 21, 49).

Eukaryotes contain the Arg/N-degron pathway (it recognizes, in particular, specific unacetylated Nt-residues) (Fig. 1), the Ac/N-degron pathway (it recognizes, in particular, the N^α-terminally acetylated [Nt-acetylated] Nt-residues), the Pro/N-degron pathway (it recognizes, in particular, the Nt-Pro residue or a Pro at position 2), the Gly/N-degron pathway (it recognizes Nt-Gly), and the fMet/N-degron pathway (it recognizes proteins that had been "pretranslationally" Nt-formylated) (*SI Appendix, Fig. S1*) (2, 9, 10, 22–24, 26, 27, 46–48, 50).

Most N-degrons are initially cryptic (pro-N-degrons). They become active N-degrons either constitutively (e.g., cotranslationally) or via regulated steps. Nonprocessive proteases, including caspases, calpains, separases, and cathepsins, act as specific components of N-degron pathways, since a cleavage of a protein can generate a C-terminal (Ct) fragment bearing an N-degron (9, 10, 33, 46, 51, 52). Active N-degrons can also be formed through enzymatic Nt-acetylation, Nt-deamidation, Nt-oxidation, Nt-arginylation, Nt-leucylation, and Nt-formylation of specific proteins (Fig. 1 and *SI Appendix, Fig. S1*). Recognition components of N-degron pathways are called N-recognins. They are E3 Ub ligases or other proteins, for example, mammalian p62 or bacterial ClpS, that can recognize N-degrons (2, 6, 9, 10, 23, 24, 41). In cognate sequence contexts, all 20 amino acids of the genetic code are capable of functioning as destabilizing Nt-residues (*SI Appendix, Fig. S1*). Consequently, many proteins in a

Significance

The Arg/N-degron pathway targets proteins for degradation by recognizing their N-terminal residues. In the present study, we used *in vivo* and *in vitro* binding assays to identify specific multienzyme targeting complexes of the Arg/N-degron pathway in yeast (*Saccharomyces cerevisiae*) and human cells. These targeting complexes contain N-terminal amidases, an arginyltransferase, and specific ubiquitin ligases of the Arg/N-degron pathway. Enzymes or assemblies of enzymes that catalyze sequential reactions have been observed to exhibit substrate channeling, in which a reaction intermediate can be transferred between active sites of interacting enzymes without release of intermediate to the bulk solution. It remains to be determined whether targeting complexes discovered in the present work function to enable substrate channeling.

Author contributions: J.-H.O., J.-Y.H., S.-J.C., and A.V. designed research; J.-H.O., J.-Y.H., and S.-J.C. performed research; J.-H.O., J.-Y.H., S.-J.C., and A.V. analyzed data; and J.-H.O., J.-Y.H., S.-J.C., and A.V. wrote the paper.

Reviewers: T.A., University of Bergen; and W.P.T., Vanderbilt University.

The authors declare no competing interest.

Published under the [PNAS license](#).

¹To whom correspondence may be addressed. Email: avarsh@caltech.edu.

This article contains supporting information online at <https://www.pnas.org/lookup/suppl/doi:10.1073/pnas.2003043117/-DCSupplemental>.

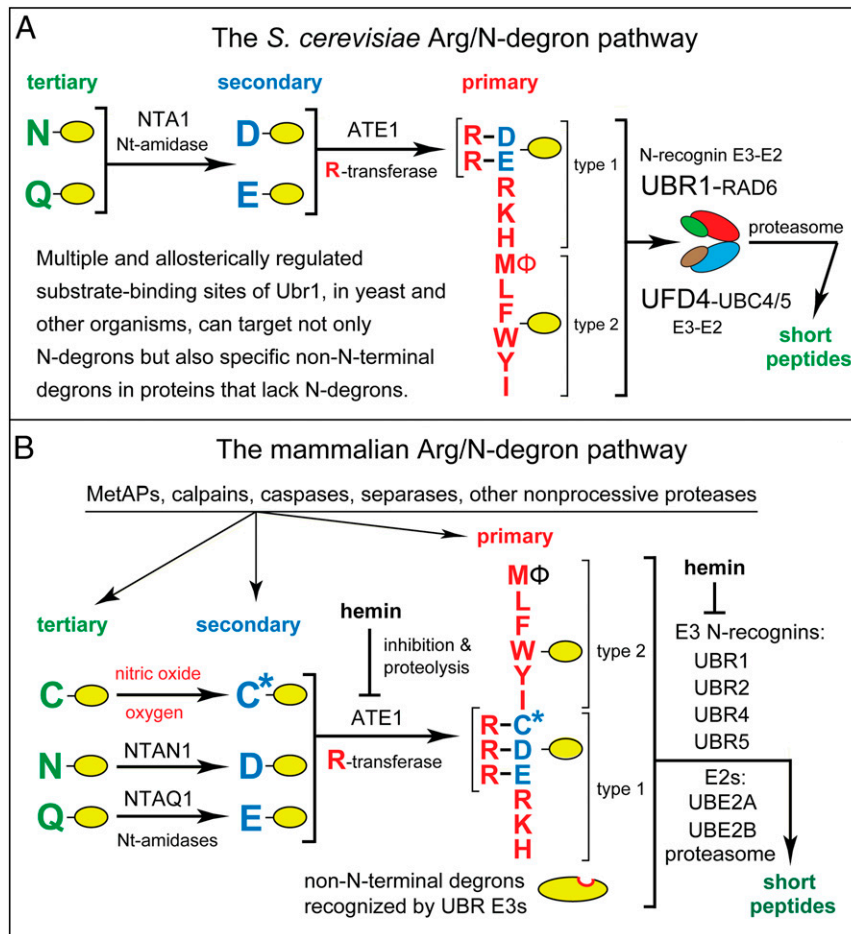


Fig. 1. (A) The *S. cerevisiae* Arg/N-degron pathway. Nt-residues are denoted by single-letter abbreviations. Yellow ovals denote the rest of a protein substrate. "Primary," "secondary," and "tertiary" refer to mechanistically distinct classes of destabilizing Nt-residues. "Type 1" and "type 2" refer, respectively, to two sets of primary destabilizing Nt-residues, basic (Arg, Lys, His) and bulky hydrophobic (Leu, Phe, Trp, Tyr, Ile, and also Met, if the latter is followed by a bulky hydrophobic residue [Φ]). These Nt-residues are recognized by two substrate-binding sites (type 1 and type 2) of *sc*UBR1, the pathway's E3 N-recognin. (B) The mammalian Arg/N-degron pathway. Hemin (Fe^{3+} -heme) inhibits the activity of R-transferase and accelerates its degradation in vivo. Hemin also binds to UBR1/UBR2 E3s and inhibits specific aspects of their activity (2, 22, 24). Besides recognizing Arg/N-degrons, E3s of the Arg/N-degron pathway contain, in addition, specific binding sites that are exposed conditionally and recognize non-Nt degrons of proteins that lack Arg/N-degrons (2, 9, 22, 24). See Introduction for references and other details. See also *SI Appendix, Fig. S1* for other N-degron pathways.

cell are constitutive or conditional N-degron substrates, either as full-length proteins or as Ct-fragments.

Regulated degradation of proteins or their natural fragments by N-degron pathways has been shown to function in a large number of biological processes, including the sensing of short peptides, heme, oxygen, and nitric oxide (NO); the regulation of subunit stoichiometries in oligomeric proteins; the elimination of misfolded proteins; the control of DNA repair, transcription, replication, and chromosome cohesion/segregation; the regulation of G proteins, chaperones, cytoskeletal proteins, gluconeogenesis, autophagy, peptide transport, meiosis, circadian rhythms, cell migration, fat metabolism, immunity (including inflammation), cardiovascular system, neurogenesis, and spermatogenesis; a suppression of neurodegeneration and regulation of apoptosis; and also plant cell differentiation, plant defenses against pathogens, the sensing of oxygen and NO, and many other processes in plants (refs. 2, 9, 10, 20, 22–32, 34, 36–47, 50, 53–57, and references therein).

To keep notations uniform, human genetic terms (all-uppercase letters) are used below to denote both human (*Homo sapiens*, *hs*) and yeast (*Saccharomyces cerevisiae*, *sc*) genes and proteins. *sc*UBR1 encodes the 225-kDa RING-type E3, denoted as *sc*UBR1, that functions as the sole N-recognin of the *S. cerevisiae* Arg/

N-degron pathway. Unmodified Nt-Arg, Nt-Lys, Nt-His, Nt-Leu, Nt-Phe, Nt-Tyr, Nt-Trp, Nt-Ile, and Nt-Met (if Met is followed by a bulky hydrophobic residue) are "primary" destabilizing Nt-residues in that they are directly bound by *sc*UBR1 (Fig. 1A) (2, 20, 22, 33, 34, 36, 51, 58–60). In contrast, Nt-Asp and Nt-Glu are destabilizing because of their Nt-arginylation by *sc*ATE1 arginyltransferase (R-transferase). The resulting (conjugated) Nt-Arg is bound by *sc*UBR1. Nt-Asn and Nt-Gln are destabilizing since *sc*NTA1 Nt-amidase converts them to Nt-arginylatable Nt-Asp and Nt-Glu (Fig. 1A) (61, 62). *sc*UBR1 E3 contains multiple binding sites that can target not only N-degrons but also other degrons in specific N-degron-lacking proteins (9, 57, 63, 64). *sc*UBR1 E3 is bound to its cognate E2 (Ub-conjugating) enzyme *sc*RAD6, and also to a complex of *sc*UFD4 E3 with its cognate E2 enzyme (*sc*UBC4 or *sc*UBC5) (Fig. 1A) (65).

In contrast to *S. cerevisiae*, the human genome encodes at least four N-recognin E3s, the 200-kDa *hs*UBR1 and *hs*UBR2, the 570-kDa *hs*UBR4 (p600, BIG), and the 300-kDa *hs*UBR5 (EDD1, HYD) (Fig. 1B) (2, 24, 66–68). Yet another N-recognin of the human Arg/N-degron pathway is p62, an autophagy-regulating protein distinct from E3s (41, 69, 70). *hs*UBR1 and *hs*UBR2 E3s are sequelous (similar in sequence) (71) (they

are 47% identical) to each other and to *S. cerevisiae* scUBR1 (6). In contrast, sequelogies (sequence similarities[†]) between *hsUBR1/hsUBR2* and *hsUBR4* or *hsUBR5* are confined largely to their ~80-residue UBR domains, which recognize N-degrons that bear N-terminal Arg, Lys, or His (Fig. 1B) (2, 59, 60). Animals and plants contain two Nt-amidases, the Nt-Asn-specific NTAN1, and the Nt-Gln-specific NTAQ1 (47, 50, 72). At least in multicellular eukaryotes, Nt-arginylation encompasses not only Nt-Asp and Nt-Glu but also Nt-Cys, after its conditional (oxygen/NO-dependent) oxidation to Nt-Cys-sulfinate or Nt-Cys-sulfonate (Fig. 1B) (44, 47, 55, 73–75).

Degradation, by the human Arg/N-degron pathway, of a substrate bearing, for example, Nt-Asn involves deamidation of Nt-Asn by the Asn/Nt-amidase *hsNTAN1*; Nt-arginylation of resulting Nt-Asp by the *hsATE1* R-transferase; the binding of resulting (conjugated) Nt-Arg to the *hsUBR1* (or *hsUBR2*) E3 component of the E3-E2 Ub ligase; the ligase-mediated synthesis of a poly-Ub chain linked to a substrate's internal Lys residue; the capture of substrate (at least in part through its poly-Ub) by the 26S proteasome; and the substrate's processive degradation by the proteasome (Fig. 1B).

In the present study, we discovered that the Asn/Nt-amidase *hsNTAN1*, the Gln/Nt-amidase *hsNTAQ1*, the R-transferase *hsATE1*, and the E3-E2 Ub ligase *hsUBR1-hsUBE2A/B* (or *hsUBR1-hsUBE2A/B*) (Fig. 1B) form a targeting complex of the human Arg/N-degron pathway. In addition, the yeast Nt-amidase *scNTA1*, the R-transferase *scATE1*, and the double-E3 Ub ligase *scUBR1-scRAD6/scUFD4-scUBC4/5* (Fig. 1A) were found to form an analogous targeting complex of the *S. cerevisiae* Arg/N-degron pathway. Previous work by this laboratory showed that *scUBR1* and *scUFD4* E3s, which bind to each other (65), also bind to the 26S proteasome (76). That evidence, if viewed together with results of the present study, suggests an even larger N-degron-targeting complex that contains the proteasome as well.

Enzymes or assemblies of enzymes that catalyze sequential reactions have been observed to exhibit substrate channeling, in which a reaction intermediate can be transferred between active sites of interacting enzymes without release of intermediate to the bulk solution (77–85). It remains to be determined whether targeting complexes identified in the present work function to enable substrate channeling.

Specific features of protein-sized Arg/N-degron substrates and targeting complexes that capture them led us to a verifiable concept, termed “superchanneling.” This mechanism is mutually nonexclusive vis-à-vis substrate channeling. In superchanneling, the last modification of a substrate, i.e., the synthesis of a substrate-linked poly-Ub chain can bypass sequential Nt modifications of the substrate by skipping, within a targeting complex, some or all of these modifications. We discuss predictions of the superchanneling model and approaches to its verification.

Results and Discussion

Protein Binding Assays. Our previous (28, 86) and present work employed the yeast-based two-hybrid (Y2H) method of Fields and colleagues (87–89) for detecting *in vivo* protein interactions. In assays with Y2H-based protein fusions, we varied locations (Nt or Ct) of a fusion's activation domain (AD) or DNA-binding

domain (DBD), particularly if an initial Y2H assay did not detect an interaction. Controls included immunoblotting to examine Y2H-based fusions, and also verifying that binding-positive Y2H fusions were not autoactivating, i.e., that none of them were positive in Y2H assays that contained just one of two fusions. The results summarized below passed all of these controls. This study also employed split-Ub, glutathione transferase (GST)-pull-down, and coimmunoprecipitation (co-IP) binding assays (Figs. 2–5 and *SI Appendix*, Figs. S2–S10).

Human *hsUBR1* and *hsUBR2* E3s Bind to the Nt-Asn-Specific Nt-Amidase *hsNTAN1*. Y2H assays with the full-length 200-kDa *hsUBR1* E3 N-recogin vs. the Asn/Nt-amidase *hsNTAN1* revealed their interaction (Figs. 1B and 2, rows 1 to 3). Y2Hs with *hsUBR2* E3 yielded similar results, in that *hsUBR2* also interacted with *hsNTAN1* (*SI Appendix*, Fig. S2, rows 1 to 3).

Human *hsUBR1* and *hsUBR2* E3s Bind to the Nt-Gln-Specific Nt-Amidase *hsNTAQ1*. Nt-amidases catalyze similar reactions (Fig. 1). Nevertheless, the human Asn/Nt-amidase *hsNTAN1* is not sequelogous to either the human Gln/Nt-amidase *hsNTAQ1* or the *S. cerevisiae* Nt-amidase *scNTA1*, which can deamidate both Nt-Asn and Nt-Gln (47, 50, 62, 72). The absence of sequelogy suggests independent evolutionary origins of the three Nt-amidases. Y2Hs indicated the binding of both *hsNTAQ1* and *hsNTAN1* to both *hsUBR1* E3 and *hsUBR2* E3 (Figs. 1B and 2, rows 1 to 6, and *SI Appendix*, Fig. S2, rows 1 to 9, *SI Appendix*, Fig. S5, row 1, and *SI Appendix*, Fig. S6, row 17).

To address these interactions in a different way, we also used GST-pull-down assays (64, 90). GST alone as well as *hsNTAN1*-GST and GST-*hsNTAQ1* fusions were expressed in *Escherichia coli*, purified, and immobilized on glutathione-Sepharose beads (*SI Appendix*, Fig. S9 A and B). Equal amounts of extract from *S. cerevisiae* that expressed the N-terminally flag-tagged human

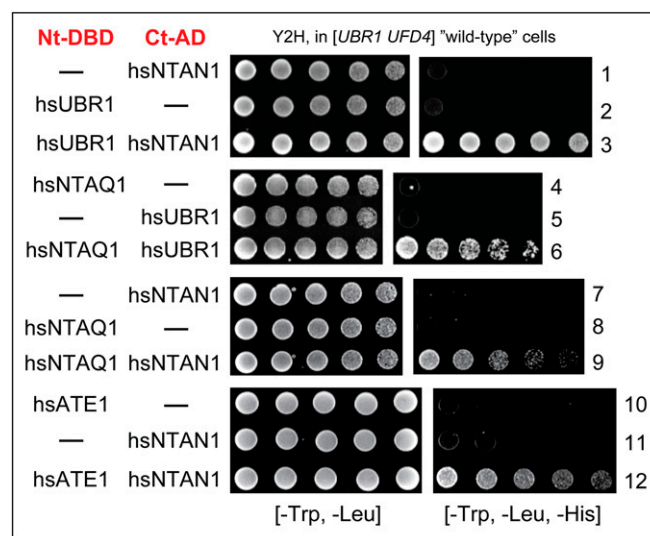


Fig. 2. Y2H binding assays, in wild-type (*UBR1 UFD4*) *S. cerevisiae*, with enzymes of the human Arg/N-degron pathway. Expression of *HIS3*, the assays' readout in otherwise His⁻ cells, is a function of binding affinity between test proteins (87). Histidine-lacking plates (shown on the right) were incubated for ~2 d at 30 °C to detect the growth of His⁺ cells. Nt and Ct Y2H-specific domains in Y2H-based protein fusions are marked in red. Row 1, *hsNTAN1* vs. vector alone. Row 2, *hsUBR1* vs. vector alone. Row 3, *hsUBR1* vs. *hsNTAN1*. Row 4, *hsNTAQ1* vs. vector alone. Row 5, *hsUBR1* vs. vector alone. Row 6, *hsNTAQ1* vs. *hsUBR1*. Row 7, *hsNTAN1* vs. vector alone. Row 8, *hsNTAQ1* vs. vector alone. Row 9, *hsNTAN1* vs. *hsNTAQ1*. Row 10, *hsATE1* vs. vector alone. Row 11, *hsNTAN1* vs. vector alone. Row 12, *hsATE1* vs. *hsNTAN1*. See also *SI Appendix*, *Materials and Methods*.

[†]"Sequelog" denotes a sequence that is similar, to a specified extent, to another sequence (71). Derivatives of sequelog include "sequelogy" (sequence similarity) and "sequelogenous" (similar in sequence). The usefulness of sequelog and derivative notations stems from the rigor and clarity of their evolutionary neutrality. In contrast, in settings that use "homolog," "ortholog," and "paralog" (they denote, respectively, common descent and functional similarity/dissimilarity), these terms are often interpretation-laden and can be imprecise. Homolog, ortholog, and paralog are compatible with the sequelog terminology. The former terms can be used to convey understanding about common descent and biological functions, if this additional information, distinct from sequelogy per se, is actually present (71).

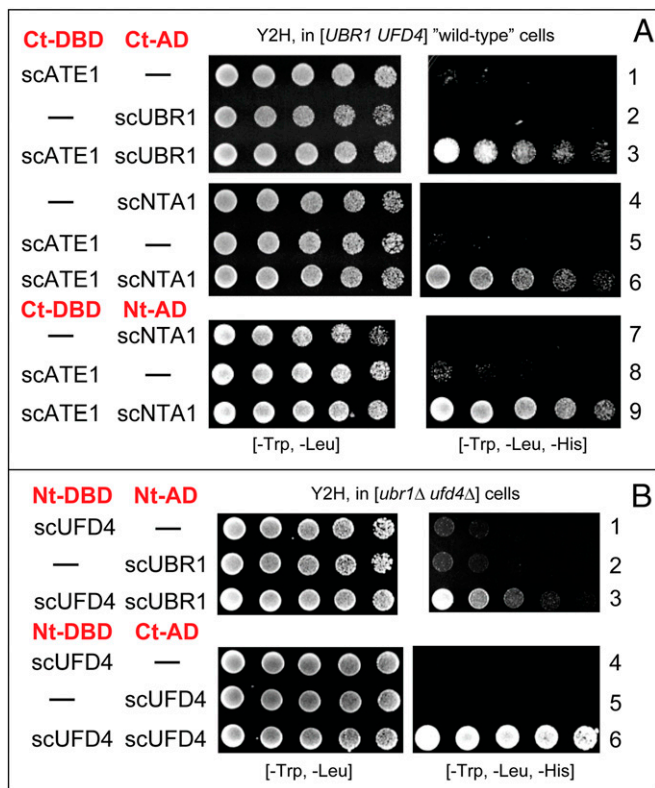


Fig. 3. Y2H binding assays with enzymes of the *S. cerevisiae* Arg/N-degron pathway. (A) Y2Hs in wild-type (*UBR1 UFD4*) *S. cerevisiae*. Row 1, scATE1 vs. vector alone. Row 2, scUBR1 vs. vector alone. Row 3, scATE1 vs. scUBR1. Row 4, scNTA1 vs. vector alone. Row 5, scATE1 vs. vector alone. Row 6, scATE1 vs. scNTA1. Row 7, scNTA1 vs. vector alone. Row 8, scATE1 vs. vector alone. Row 9, scATE1 vs. scNTA1. (B) Y2Hs in [*ubr1Δ ufd4Δ*] *S. cerevisiae*. Row 1, scUFD4 vs. vector alone. Row 2, scUBR1 vs. vector alone. Row 3, scUFD4 vs. scUBR1. Row 4, scUFD4 (Nt-DBD-tagged) vs. vector alone. Row 5, scUFD4 (Ct-AD-tagged) vs. vector alone. Row 6, scUFD4 vs. scUFD4. See also the legend to Fig. 2 and *SI Appendix, Materials and Methods*.

$f_{hs}UBR2$ E3 were incubated with the above (preloaded on beads) GST or GST fusions, followed by washes, elution of beads-associated proteins, their SDS/PAGE, and immunoblotting for $f_{hs}UBR2$ with anti-flag antibody. In agreement with the above Y2H results, $f_{hs}UBR2$ interacted with both *hsNTAN1*-GST and GST-*hsNTAQ1*, but did not bind to GST alone (Fig. 4D).

The Human Asn/Nt-Amidase *hsNTAN1* Binds to the Gln/Nt-Amidase *hsNTAQ1*. In addition to their binding to the *hsUBR1* (and *hsUBR2*) E3 Ub ligases, the *hsNTAN1* and *hsNTAQ1* Nt-amidases were also found to interact with each other, in the absence of both *hsUBR1* and *hsUBR2* (Fig. 2, rows 7 to 9). On the assumption (it remains to be verified) that pairwise interactions among *hsNTAN1*, *hsNTAQ1*, and *hsUBR1* (or *hsUBR2*) are mutually nonexclusive, these binding modes would be multivalent and would be expected, therefore, to increase the overall stability of the tripartite *hsNTAN1*-*hsNTAQ1*-*hsUBR1* complex, in comparison to pairwise interactions within the complex (Fig. 6A).

The Human *hsATE1* R-Transferase Binds to *hsNTAN1* Asn/Nt-Amidase. ATE1 R-transferase conjugates Arg to Nt-Asp, Nt-Glu, or oxidized Nt-Cys. The R-transferase branch of the Arg/N-degron pathway is a sensor of oxygen and NO in animals and plants (*Introduction* and Fig. 1B) (44, 73, 74, 91, 92). Using Y2H-based *hsATE1* fusions (tagged with Nt-DBD or Ct-DBD domains), we found that

hsATE1 R-transferase binds to *hsNTAN1* Asn/Nt-amidase (Fig. 2, rows 10 to 12, and *SI Appendix, Fig. S2*, rows 13 to 15).

The Human *hsATE1* R-Transferase Does Not Bind to *hsNTAQ1* Gln/Nt-Amidase. In contrast to the binding of *hsATE1* R-transferase to Asn/Nt-amidase *hsNTAN1* (see above), Y2Hs were negative with *hsATE1* vs. Gln/Nt-amidase *hsNTAQ1*. These results are shown here for Nt-DBD/*hsNTAQ1* vs. Nt-AD/*hsATE1* (*SI Appendix, Fig. S2*, rows 10 to 12), and similar results (no interaction) were obtained with all eight Nt/Ct permutations of the DBD and AD domains linked to *hsNTAQ1* and *hsATE1*.

To address this question in a different way, we used a yeast-based split-Ub assay (93, 94). In split-Ub, proteins are expressed as fusions, respectively, to a Ct-half of Ub (C_{Ub}) and to its mutant Nt-half (N_{Ub}). Interactions between test proteins would reconstitute a quasi-native Ub moiety from C_{Ub} and mutant N_{Ub} , causing the cleavage of a C_{Ub} -containing fusion by deubiquitylases downstream from (reconstituted) Ub moiety. Through additional steps, this cleavage acts as readout of split-Ub assays (93, 94). In agreement with Y2H assays (*SI Appendix, Fig. S2*, rows 10 to 12), split-Ub (using two orientations of test proteins vis-à-vis N_{Ub} and C_{Ub}) was negative with *hsATE1* vs. *hsNTAQ1* (*SI Appendix, Fig. S8*).

Engineered Yeast Strains That Coexpress Human Proteins: *hsATE1* R-Transferase Binds to *hsUBR2* E3. Y2Hs with *hsATE1* vs. full-length *hsUBR1* E3 or Nt-half of *hsUBR2* (*hsUBR2*¹⁻¹⁰⁴⁰) did not detect their binding to *hsATE1* (*SI Appendix, Fig. S4*, rows 1 to 6). Given these findings, and given Y2H-positive (i.e., the opposite) results with *S. cerevisiae* scATE1 vs. scUBR1 (see below), we used co-IP to address a possible interaction between *hsATE1* and *hsUBR2* that might have escaped detection by Y2H.

To carry out co-IP assays, we constructed *S. cerevisiae* strains in which cDNAs encoding five components of the human Arg/N-degron pathway were integrated into the yeast genome downstream from constitutive or galactose-inducible promoters (*SI Appendix, Fig. S10*). These strains expressed specific combinations of five human proteins, tagged with different epitopes ($^{3f}hsUBR2$, $^{3hsv}hsATE1$, *hsNTAN1*^{3ha}, $^{3myc}hsNTAQ1$, *hsUBE2B*), and one strain expressed all five human proteins, as determined by SDS/PAGE and immunoblotting with five different antibodies (Fig. 4A and B and *SI Appendix, Table S1*). Untagged *hsUBE2B* E2 was detected using an antibody to *hsUBE2B* (Fig. 4B).

In one example of this approach, we used *S. cerevisiae* that expressed two (and only two) human proteins, $^{3f}hsUBR2$ E3 and $^{3hsv}hsATE1$ R-transferase (Fig. 4A, lane 3). IP of extract from these cells was carried out using anti-hsv antibody to $^{3hsv}hsATE1$. SDS/PAGE of anti-hsv-precipitated proteins, followed by immunoblotting with anti-flag antibody (specific, in this setting, for $^{3f}hsUBR2$), detected coimmunoprecipitated $^{3f}hsUBR2$ (Fig. 4C, lanes 2 to 4). This assay was also used with an *S. cerevisiae* strain that expressed all five components of the human Arg/N-degron pathway, with the same results (Fig. 4A, lane 9, and Fig. 4C, lanes 5 to 7).

Note that while the results of co-IP with yeast expressing solely $^{3f}hsUBR2$ and $^{3hsv}hsATE1$ (Fig. 4C, lanes 2 to 4) could be interpreted straightforwardly as evidence for interaction between *hsUBR2* and *hsATE1*, a similar co-IP finding with yeast that expressed all five human proteins (Fig. 4C, lanes 5 to 7) could also be interpreted (in the absence of evidence with the strain that expressed only two proteins) as a result that had been caused by "hitchhiking" of $^{3f}hsUBR2$ within a larger complex that contained both $^{3hsv}hsATE1$ and other coexpressed human proteins, cited in Fig. 4A and B.

A negative Y2H result, such as the one about *hsATE1* vs. *hsUBR2* (see above), does not prove the absence of binding (87–89). Therefore, we made a working assumption that a robustly positive result with co-IP assays (Fig. 4A, lane 3, and

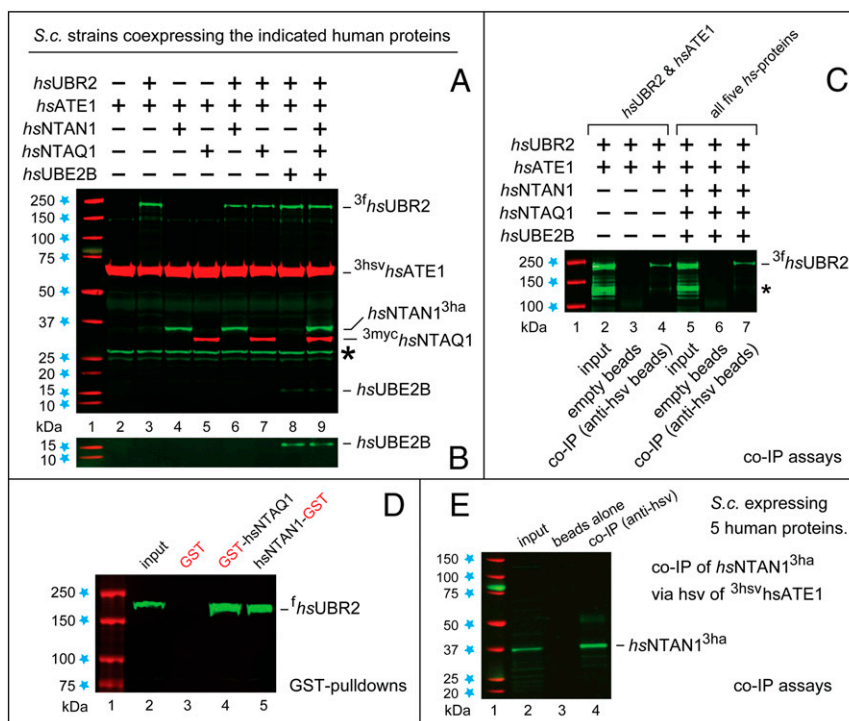


Fig. 4. Co-IPs and GST-pull-down assays with five enzymes of the human Arg/N-degron pathway. (A) Lane 1, kilodalton markers. Lanes 2 to 9, immunoblotting (using a mixture of relevant antibodies) of extracts of eight *S. cerevisiae* strains that stably coexpressed specific combinations of five human proteins (indicated on top), including a strain that coexpressed all five proteins (lane 9). Epitope tags, indicated on the right, were used to mark these proteins either N terminally or C terminally. The asterisk denotes a yeast protein that cross-reacted with an antibody in the mix. Untagged *hsUBE2B* E2 was detected by an antibody to *hsUBE2B*. Of the two highly sequelogenous (95% identical) E2s, *hsUBE2A* and *hsUBE2B*, only the latter was analyzed in this study. The indicated yeast strains were constructed as described in *SI Appendix, Materials and Methods* and *Fig. S10*, through site-specific integrations, into the *S. cerevisiae* genome, of human cDNAs. (B) The same as the lower part of immunoblot in A, but a higher fluorescence intensity, to increase the brightness of the *hsUBE2B* bands in lanes 8 and 9. (C) Lane 1, kilodalton markers. Lane 2, detection by immunoblotting, using anti-flag, of 3f hsUBR2 in an input sample of extract from *S. cerevisiae* that coexpressed 3f hsUBR2 and 3hsv hsATE1 (see lane 3 in A). Lanes 3 and 4, anti-hsv antibody-lacking (lane 3) and anti-hsv-containing beads (lane 4) were used to immunoprecipitate proteins in the extract, followed by SDS/PAGE and immunoblotting with anti-flag antibody. Note the band of coimmunoprecipitated 3f hsUBR2 in lane 4 but not in lane 3. Lanes 5 to 7, same as lanes 2 to 4 but with *S. cerevisiae* that coexpressed all five human proteins (see also A, lane 9). The asterisk denotes a flag-retaining proteolytic fragment of 3f hsUBR2. (D) GST-pull-down assays, with immunoblottings using anti-flag antibody. Lane 1, kilodalton markers. Lane 2, input sample of extract from *S. cerevisiae* that expressed the human f hsUBR2 E3. Lanes 3 to 5, GST pull-downs with test proteins immobilized on glutathione beads: GST alone, GST-hsNTAQ1, and hsNTAN1-GST. Note the absence of interaction between f hsUBR2 and GST. (E) Lane 1, kilodalton markers. Lane 2, an input sample of extract from *S. cerevisiae* that coexpressed all five human proteins, including 3hsv hsATE1 (see also A, lane 9, and C, lanes 5 to 7), was fractionated by SDS/PAGE and analyzed by immunoblotting with anti-ha antibody to 3ha hsNTAN1. Lanes 3 and 4, anti-hsv antibody-lacking (lane 3) and anti-hsv-containing beads (lane 4) were used, respectively, to immunoprecipitate proteins in the extract, followed by SDS/PAGE and immunoblotting with anti-ha antibody. Note the band of co-IP 3ha hsNTAN1 in lane 4 but not in lane 3.

Fig. 4C, lanes 2 to 4) was likely to signify a bona fide interaction between *hsATE1* and *hsUBR2*, while noting the absence of agreement, in this (and only this) case, between Y2H and co-IP assays.

Another example of this co-IP approach, with the yeast strain that expressed just two human proteins, 3f hsUBR2 E3 and its cognate E2 enzyme *hsUBE2B*, was detection of interaction between these enzymes (*SI Appendix, Fig. S9C*).

Yet another example of co-IP approach was IP of extract from the yeast strain that coexpressed all five human proteins (Fig. 4A, lane 9). The result was detection, in an 3hsv hsATE1-specific anti-hsv immunoprecipitate, of the coimmunoprecipitated *hsNTAN1*^{3ha} Asn/Nt-amidase (Fig. 4E). Considered together, co-IP data indicated that the 3hsv hsATE1-specific anti-hsv immunoprecipitate contained at least 3hsv hsATE1, *hsNTAN1*^{3ha}, 3f hsUBR2, and *hsUBE2B*, a glimpse of binding patterns beyond pairwise interactions (Figs. 4A–C and E and 6A and *SI Appendix, Fig. S9C*). A “complete” targeting complex remains to be characterized in vivo and reconstituted in vitro.

hsTRIP12, a Human Sequelogue of the Yeast *scUFD4* E3, Does Not Bind to *hsUBR1*. Previous work has shown that *scUBR1*, the 225-kDa RING-type E3 N-recogin, binds to *scUFD4*, a 168-kDa HECT-

type E3 (Fig. 1A) (65). *scUBR1* and *scUFD4* function as the double-E3 *scUBR1/scRAD6-scUFD4/scUBC4/5* E3-E2 Ub ligase (65). One function of *scUFD4* (which is not an N-recogin) is to increase the length of a substrate-linked poly-Ub chain that has been initiated by *scUBR1* (65, 95).

The closest human sequelogue of the *S. cerevisiae* *scUFD4* E3 is *hsTRIP12* E3 (96–99). *scUFD4* and *hsTRIP12* are 23% identical and 53% similar. However, Y2Hs did not detect an interaction between *hsTRIP12* and *hsUBR1* (*SI Appendix, Fig. S4*, rows 7 to 9). Since negative Y2H results are not definitive (87–89), a potential role of *hsTRIP12* in the human Arg/N-degron pathway remains to be addressed. With this caveat, *hsTRIP12* is apparently not a part of the human targeting complex, in contrast to *S. cerevisiae*, in which *scUBR1* binds to *scUFD4* (65) (Fig. 3, rows 1 to 3).

The Human Cys-Dioxygenase *hsADO* Does Not Bind to *hsUBR1*, *hsUBR2*, and *hsATE1*. In animals and plants, Nt-Cys of some Nt-Cys-bearing proteins can be oxidized through oxygen/NO-dependent reactions, yielding Nt-Cys-sulfinate or Nt-Cys-sulfonate (Nt-Cys*). Nt-arginylation, by ATE1 R-transferase, of (oxidized) Nt-Cys* in mammalian proteins that include G protein regulators RGS4, RGS5, and RGS16, and in specific transcription

Pairwise interactions in the human targeting complex

human proteins	NTAN1	NTAQ1	ATE1	UBR1/2	UBE2
NTAN1	● —	●● +	●●● +	●●● +	nd
NTAQ1	● +	●● +	●●● —	●●● +	nd
ATE1	● +	● —	●●● —	●●● +	nd
UBR1/2	● +	● +	● —	●●● —	● +
UBE2	● +	● +	● —	● —	● +

● Y2H; ● split-Ub; ● GST-pulldowns; ● co-IP

Fig. 5. Summary of binding assays and detected pairwise interactions among five enzymes of the human Arg/N-degron pathway. Plus and minus signs indicate, respectively, a detected interaction between two indicated human proteins, and the apparent absence of binding. nd, not determined. Colored circles denote in vivo Y2H assays, in vivo split-Ub assays, in vitro GST-pulldown assays, and in vitro co-IP assays, used with the indicated pairs of proteins. In the sole case of disagreement between results of two different assays, the binding of *hsATE1* to *hsUBR2* was detected by co-IP but was not detected by Y2Hs (Fig. 4C and *SI Appendix*, Fig. S4, rows 1 to 6). The use, in this study, of more than one binding assay vis-à-vis a given pair of proteins was extensive but not exhaustive.

factors of plants results in degradation of these proteins by the Arg/N-degron pathway (2, 44, 73, 74, 100, 101). This pathway is thus a sensor of oxygen and NO and regulator of responses to these compounds (2, 100). Oxidation of Nt-Cys is mediated, at least in part, by Nt-Cys dioxygenases (2-aminoethanol dioxygenases) such as *hsADO* (44, 101). We used Y2H to ask whether *hsADO* Nt-Cys-dioxygenase might interact with *hsUBR1* or *hsUBR2* E3s, or with *hsATE1* R-transferase. The results were negative (*SI Appendix*, Fig. S5), suggesting (but not proving) that *hsADO* dioxygenase is not a part of the human Arg/N-degron-targeting complex.

The Human Arg-tRNA Synthetase Does Not Bind to *hsUBR2* and *hsATE1*. R-transferase is a part of the human Arg/N-degron-targeting complex (Figs. 5 and 6). Since Arg-tRNA is a cosubstrate of *hsATE1* (2), and since fractionations of mammalian cell extracts suggested the possibility of a complex between R-transferase and Arg-tRNA synthetase (102), we used Y2Hs to ask whether the cytosolic Arg-tRNA synthetase *hsRARS* might bind to *hsATE1* R-transferase or *hsUBR2* E3. Negative results of these Y2H assays (*SI Appendix*, Fig. S6) suggested (but did not prove) that there is no interaction between *hsRARS* and either *hsATE1* or *hsUBR2*.

Self-Interactions Among Components of the Human Targeting Complex. We also asked whether *hsNTAQ1*, *hsNTAN1*, and *hsATE1* (Fig. 1B) might self-interact (e.g., homodimerize). The results were positive for Gln/Nt-amidase *hsNTAQ1*, but negative for Asn/Nt-amidase *hsNTAN1* and *hsATE1* R-transferase (Fig. 5 and *SI Appendix*, Fig. S7). As described above, *hsNTAQ1* and

hsNTAN1 bind to each other, and both of them also bind to *hsUBR1* (and *hsUBR2*) E3 (Figs. 2 and 4–7, *SI Appendix*, Fig. S2 and *SI Appendix*, S5, row 1). In the crystal structure of human

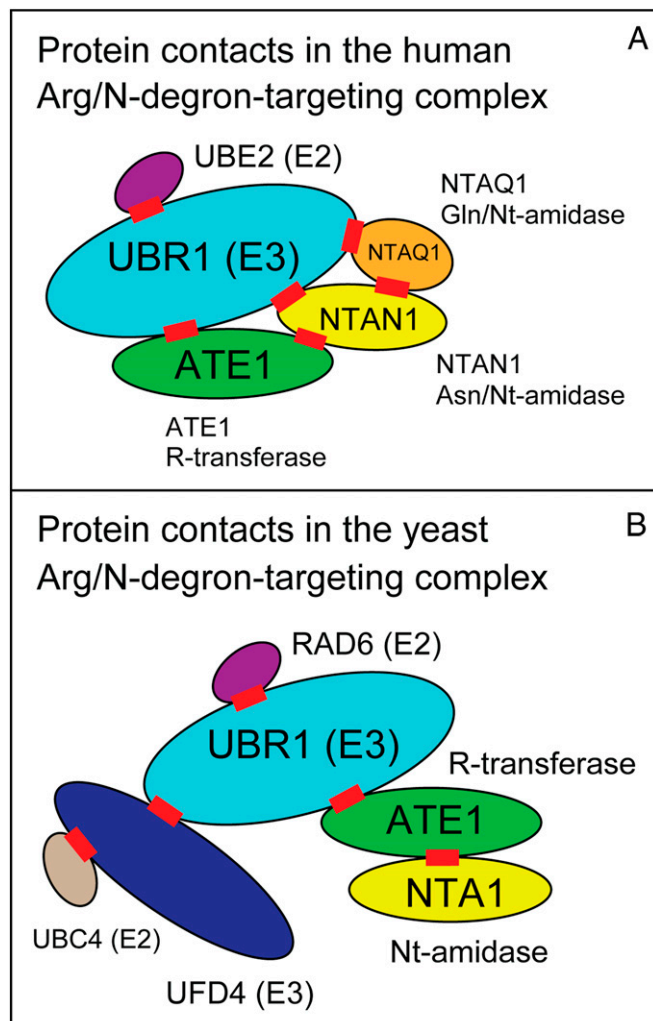


Fig. 6. Diagram of detected contacts (interactions) among subunits of the human and *S. cerevisiae* targeting complexes in the Arg/N-degron pathway. In *A* and *B*, each red rectangle denotes a detected interaction between a pair of subunits. All subunits are shown as ovals whose relative sizes are roughly proportional to subunits' molecular masses. Specific locations of protein contacts (red rectangles) within subunits [including E3-E3 contacts in *B* (65)] are largely unknown and are placed arbitrarily. [One partially defined interaction interface is between the polyacidic Ct-region of scRAD6 E2 and the basic residue-rich region of scUBR1 E3 (109).] Since some proteins in these complexes were found to self-interact in pairwise binding assays (see *Results and Discussion*), the stoichiometries of subunits in these complexes are known only in part. The depicted pairwise interactions in *A* and *B* are also underlain by the assumption that none of these contacts are mutually exclusive. (A) The human targeting complex: The 200-kDa *hsUBR1* (or *hsUBR2*) E3 enzyme, the 17-kDa *hsUBE2B* (or *hsUBE2A*) E2 enzyme, the 57-kDa *hsATE1* R-transferase, the 34-kDa *hsNTAN1* Asn/Nt-amidase, and the 23-kDa *hsNTAQ1* Gln/Nt-amidase. Pairwise interactions identified in the present study are those of *hsUBR1* (or *hsUBR2*) with *hsNTAN1*, *hsNTAQ1*, *hsATE1*, and *hsUBE2B*, as well as those of *hsNTAN1* with *hsNTAQ1* and *hsATE1* (see *Results and Discussion* and Fig. 5). (B) The *S. cerevisiae* targeting complex: The 50-kDa scNTA1 Asn/Gln/Nt-amidase, the 55-kDa scATE1 R-transferase, the 225-kDa scUBR1 E3, the 168-kDa scUFD4 E3, the 19-kDa scRAD6 E2, and the 16-kDa scUBC4 (or scUBC5) E2. Pairwise interactions identified in the present study are those of scUBR1 with scNTA1, and of scNTA1 with scATE1 (see *Results and Discussion*). Three-dimensional crystal structures are known for *hsNTAQ1* Nt-amidase (72, 75), *hsNTAN1* Nt-amidase (47), scNTA1 Nt-amidase (62), scRAD6 E2 (110), and scUBC4 E2 (111).

hsNTAQ1, an extended Nt-region of one *hsNTAQ1* molecule in a crystal interacts with the substrate-binding cleft of adjacent *hsNTAQ1* molecule (75), suggesting a homodimer. Given multiple pairwise interactions among specific enzymes of the present study, a functional understanding of *hsNTAQ1* self-binding (*SI Appendix*, Fig. S7, rows 1, 2, and 6 to 8) would require structural analyses of *hsNTAQ1* as a part of the Arg/N-degron-targeting complex. One possibility is that *hsNTAQ1* forms a homodimer in the absence of *hsNTAN1*, whereas the presence of *hsNTAN1* may lead, preferentially, to the also observed *hsNTAQ1*–*hsNTAN1* heterodimer (Fig. 2, rows 7 to 9).

The Yeast Nt-Amidase *scNTA1* Binds to *scATE1* R-Transferase but Not to *scUBR1* E3. We asked whether the *S. cerevisiae* Arg/N-degron-targeting complex may be larger than the previously identified *scUBR1*/*scRAD6*–*scUFD4*/*scUBC4/5* complex, in which two interacting E3s are bound to their respective E2 enzymes (65, 103). *scNTA1*, encoding the Asn/Gln/Nt-amidase, contains Met AUG codons at positions 1 and 11. The sequence of *scNTA1* before Met¹¹ is similar to a typical mitochondrial presequence, in agreement with the presence of

scNTA1 in both the cytosol/nucleus and mitochondrial matrix (61, 62, 104). Y2Hs detected the binding of *scATE1* R-transferase to *scNTA1* Nt-amidase (the cytosolic version of it, initiated at Met¹¹). This interaction was observed with two configurations of Y2H-based *scNTA1* fusions (Fig. 3A, rows 4 to 9). Y2Hs did not detect the binding of *scNTA1* to *scUBR1* E3, in all eight Nt/Ct permutations of the DBD and AD domains linked to *scNTA1* and *scUBR1* (*SI Appendix*, Fig. S3A, rows 1 to 6).

The Yeast *scATE1* R-Transferase Binds to *scUBR1* E3. Y2Hs detected the binding of *scATE1* to *scUBR1* (Fig. 3A, rows 1 to 3). Thus, although the *scNTA1* Nt-amidase apparently does not interact directly with *scUBR1* (see above), *scNTA1* would still be expected to be a part of the targeting complex, since *scNTA1* binds to *scATE1* R-transferase (Fig. 3A, rows 4 to 9), and the latter, in turn, binds to *scUBR1* (Fig. 3A, rows 1 to 3, and Fig. 6B).

The Yeast *scUFD4* E3 Binds to the *scUBR1* E3 N-Recognin. Previous work, mentioned above, used split-Ub and co-IP binding assays to discover the functionally relevant double-E3 complex

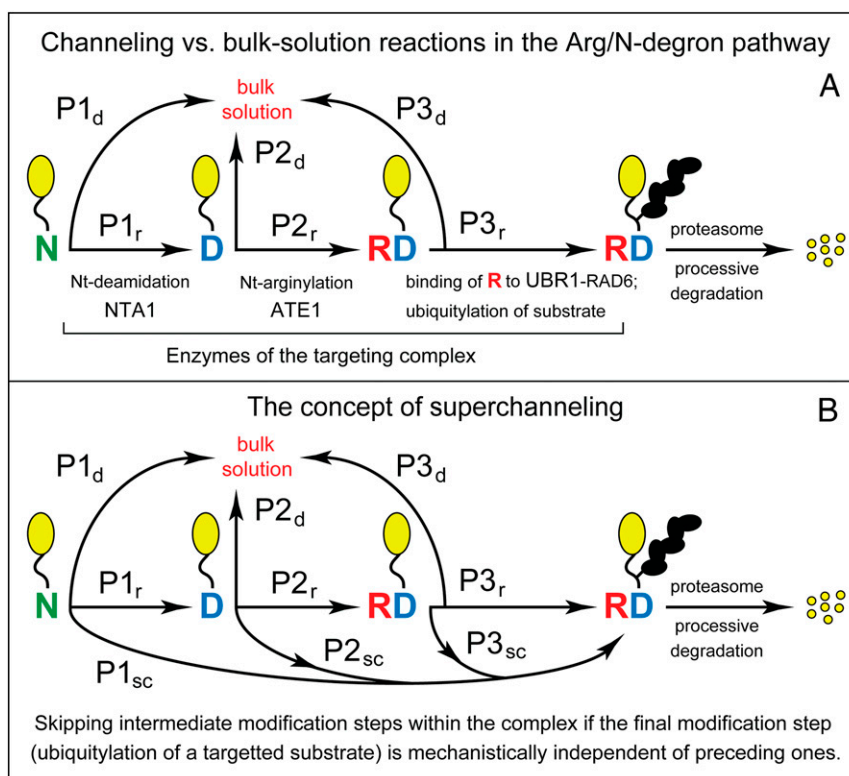


Fig. 7. The possibilities of substrate channeling and superchanneling by targeting complexes of the Arg/N-degron pathway. Shown here are diagrams for reactions mediated by the *S. cerevisiae* Arg/N-degron-targeting complex (Fig. 6B). The setting of the human complex (Fig. 6A) is similar. To simplify diagrams, we left aside (as discussed in *Results and Discussion*) the *scUFD4*–*scUBC4/5* part of the yeast targeting complex (*scUFD4* E3 is not an N-recognin). (A) Substrate channeling. Nt-residues are denoted by single-letter abbreviations. Yellow ovals denote the rest of a protein substrate. A chain of black ovals is a substrate-linked poly-Ub chain. The hypothetical possibility of substrate channeling is diagrammed as a sequence of reaction/relocation steps for an (initially) Nt-Asn-bearing substrate. The substrate is sequentially Nt-deamidated, then Nt-arginylated, then relocates and binds, via its conjugated Nt-Arg residue, to *scUBR1*–*scRAD6* E3-E2, and is polyubiquitylated by this Ub ligase, followed by the proteasome-mediated degradation of substrate. The diagram uses notations of transition probabilities, at each reaction/relocation step, for a molecule of an (initially) Nt-Asn-bearing substrate. P1_r, P2_r, and P3_r denote the probabilities of substrate moving through each reaction/relocation step while being retained (“r”) within the targeting complex (Fig. 6B). P1_d, P2_d, and P3_d denote the “alternative” probabilities of substrate’s dissociation (“d”), at each reaction/relocation step, into the bulk solution. An efficacious (as distinguished from weak or nonexistent) substrate channeling would obtain, in this setting, if P1_d << P1_r, P2_d << P2_r, and P3_d << P3_r. (B) Superchanneling. In the hypothetical concept of superchanneling (see *Results and Discussion*), the transitions (and associated probabilities) that are shown in A are “supplemented” with probabilities of superchanneling (“sc”) transitions (P1_{sc}, P2_{sc}, and P3_{sc}) at each reaction/relocation step. These transitions would result, at each step, in a bypass of downstream steps and direct polyubiquitylation of the substrate. In the language of probability-based transitions, an efficacious superchanneling would obtain, for example, if P1_r << P1_{sc} and P1_d << P1_{sc}; that is, if the initial binding of an Nt-Asn-bearing substrate to the complex-bound *scNTA1* Nt-amidase would be rapidly followed by substrate’s polyubiquitylation, without the necessity of (mechanistically independent) Nt modifications and accompanying physical relocations of the substrate. Superchanneling would not occur if P1_{sc}, P2_{sc}, and P3_{sc} are negligible in comparison to corresponding P1_r and P1_d probabilities.

scUBR1-scRAD6/scUFD4-scUBC4/5 (65). We used Y2H assays [not employed in the earlier study (65)] to confirm the binding of *scUBR1* to *scUFD4* in double-mutant [*ubr1Δ ufd4Δ*] *S. cerevisiae* that lacked the endogenous forms of these yeast E3s, thereby precluding the possibility of effects by endogenous *scUBR1/scUFD4* (Fig. 3B, rows 1 to 3).

The Yeast *scUBR1* E3 N-Recognin Does Not Self-Interact. Studies that used gel-filtration assays indicated that the 225-kDa *scUBR1* E3 N-recognin does not homodimerize at least in vitro (105, 106). In agreement with these results, Y2Hs with *scUBR1* vs. itself in [*ubr1Δ ufd4Δ*] cells also did not detect a self-interaction of *scUBR1* (SI Appendix, Fig. S3B, rows 10 to 12).

The Yeast *scUFD4* E3 Self-Interacts. Y2Hs with *scUFD4* vs. itself in [*ubr1Δ ufd4Δ*] *S. cerevisiae* indicated a self-interaction (presumably homodimerization) of *scUFD4* E3 (Fig. 3B, rows 4 to 6, and SI Appendix, Fig. S3B, rows 1 to 3). At the same time, both Y2Hs, split-Ub, and co-IP assays indicated that *scUFD4* E3 also binds to *scUBR1* E3 (Fig. 3B, rows 1 to 3) (65). It is unknown whether self-binding by *scUFD4* is mutually exclusive with the *scUFD4-scUBR1* interaction. Given the apparently monomeric state of *scUBR1* in the absence of *scUFD4* (105, 106) (SI Appendix, Fig. S3B, rows 10 to 12), the in vivo stoichiometry of these (interacting) E3s in the yeast Arg/N-degron-targeting complex remains to be determined (Fig. 6B).

The Yeast *scUFD4* E3 Does Not Bind to Nt-Amidase *scNTA1* and R-Transferase *scATE1*. We also used Y2Hs to ask whether *scUFD4* E3 (which binds to *scUBR1*, forming a double-E3 complex; see above) might interact with *scNTA1* Nt-amidase and *scATE1* R-transferase. Negative results (SI Appendix, Fig. S3B, rows 4 to 9) suggested (but did not prove) that there is no interaction between *scUFD4* E3 and either *scNTA1* or *scATE1*. In contrast, *scUBR1* interacts with *scATE1* (Fig. 3A, rows 1 to 3), and is therefore expected to be indirectly bound to *scNTA1* as well, since the latter interacts with *scATE1* (Fig. 3A, rows 4 to 9, and Fig. 6B).

On Substrate Channeling in the Arg/N-Degron Pathway. A likely function of the human and yeast Arg/N-degron-targeting complexes is substrate channeling, in which a reaction intermediate can be transferred between active sites of interacting enzymes without release of intermediate to the bulk solution (Figs. 6 and 7A). Potential advantages of channeling include its higher kinetic efficacy as well as protection/shielding of reactive and toxic intermediates (77–85). An example of direct channeling is tryptophan (Trp) synthase. Its two active sites are linked by an intraprotein tunnel. The product of the first catalyzed reaction, indole, diffuses through the tunnel from the first to the second active site, where Trp is formed from indole and a derivative of serine (83).

In a different setting, called proximity channeling, and possibly relevant to multienzyme complexes of Arg/N-degron pathways, two or more enzymes are spatially close (e.g., through their physical interaction), so that an intermediate produced by the first enzyme can be captured (most of the time or some of the time) by the second enzyme before the intermediate can diffuse away into the bulk solution. In some settings, a proximity channeling would be kinetically superior to a nonchanneled succession of the same reactions only if many quasi-identical complexes are spatially clustered together (81).

Aggregates of complexes are indeed observed with some multienzyme assemblies (77–85). Such aggregates include natural and dynamic associations of multiple 26S proteasome particles that occur in the bulk cytosol, inside the nucleus, and at the nuclear envelope (ref. 107 and references therein). Interestingly, the Arg/N-degron-targeting complexes described in the present

study (Fig. 6) apparently interact, through their E3s, with the 26S proteasome (76) (Introduction and Concluding Remarks). If Arg/N-degron-targeting complexes associate with naturally aggregated 26S proteasomes in vivo (this remains to be determined), such multienzyme assemblies may at least facilitate and possibly enable the still hypothetical substrate channeling function of targeting complexes in the Arg/N-degron pathway.

The Concept of Superchanneling. Specific features of targeting complexes and Arg/N-degron substrates (Figs. 1, 6, and 7) led us to a novel possibility vis-à-vis these complexes. The envisioned mechanism, termed “superchanneling,” is mutually nonexclusive vis-à-vis substrate channeling (Fig. 7B). We begin description of superchanneling by noting that previously characterized cases of substrate channeling are quite distinct from transitions that involve Nt modifications of Asn, Gln, Asp, Glu, or (oxidized) Cys, followed by downstream reactions (Fig. 1). First, an Arg/N-degron substrate is protein-sized (i.e., it's large and conformationally dynamic). Second, modification of a substrate that immediately precedes (and causes) its capture by the 26S proteasome is the formation of a poly-Ub linked to a substrate's cognate internal Lys residue. This reaction is not inherently sequential vis-à-vis the obligatorily sequential Nt modifications of, for example, an Nt-Asn-bearing substrate (Figs. 1 and 7).

Consider the *S. cerevisiae* targeting complex (Fig. 6B). [The same arguments are relevant to the human complex (Fig. 6A).] To simplify discussion, we leave aside the *scUFD4-scUBC4/5* part of the yeast complex (*scUFD4* E3 is not an N-recognin) (65). Suppose that in the (currently unknown) 3D structure of this complex, the substrate-binding sites of *scNTA1* Nt-amidase, *scATE1* R-transferase, and *scUBR1-scRAD6* E3-E2 face each other in such a way that movements of the N terminus of an (initially) Nt-Asn-bearing substrate between these sites upon a substrate's successive Nt modifications involve short distances, equal to or smaller than the sizes of protein molecules involved. These movements would culminate in relocation of the substrate's newly acquired (conjugated) Nt-Arg residue from the active site of *scATE1* R-transferase to the complex-bound *scUBR1* N-recognin E3. We suggest that this setting may enable a process termed superchanneling (Fig. 7B).

Specifically, an Nt-Asn-bearing substrate would be captured, initially, from the bulk solution by the targeting complex-bound *scNTA1* Nt-amidase (Figs. 1A and 7B). Depending on the spatial localization and conformational mobility of a substrate's cognate internal lysine (i.e., the Lys residue to be polyubiquitylated), this lysine may find itself, upon substrate's capture by Nt-amidase, in a stereo/catalytically favorable position vis-à-vis the active site of the *scRAD6* Ub-conjugating (E2) enzyme, which is bound to *scUBR1* E3 in the targeting complex (Fig. 7B). If so, successive Nt modifications of the captured substrate can proceed on their own, while the (initially) Nt-Asn-bearing substrate may be polyubiquitylated (at the above internal lysine) either immediately or at any later time after substrate's capture by the complex-bound Nt-amidase. In this case, a polyubiquitylation of the substrate would be able to bypass (i.e., would not have to wait for) either Nt modifications of the substrate or its relocation (after Nt-arginylation) to the Nt-Arg-binding domain of *scUBR1* E3 (Figs. 1A and 7B): Hence, the term superchanneling. It refers to the capture of, for example, an Nt-Asn-bearing substrate by Nt-amidase, to a bypass of Nt modifications/relocations of this substrate, to a bypass of relocation-mediated capture of Nt-arginylated substrate by E3, and also to channeling, for example, to the final modification (polyubiquitylation) of the substrate without its dissociation into the bulk solution.

In this hypothetical mechanism, a major role of the targeting complex-bound *scNTA1* Nt-amidase and *scATE1* R-transferase would be their physical affinity for their cognate Arg/N-degron substrates. This affinity may allow the complex-bound *scUBR1-scRAD6* E3-E2

to begin producing a substrate-linked poly-Ub without (necessarily) waiting for Nt modifications and relocations of a bound substrate to run their course.

The actual disposition, to be addressed experimentally, can range (depending on a specific Nt-Asn-bearing protein substrate) from complete absence of superchanneling to efficacious superchanneling. In the former case, Nt modifications of a substrate and relocation of the resulting Nt-Arg to E3 N-recognition would have to precede the substrate's polyubiquitylation. In the latter case, polyubiquitylation of a substrate may become stereo/catalytically feasible immediately after its capture by the complex-bound Nt-amidase (Fig. 7B).

The efficacy of classic substrate channeling would be determined by the rates of individual reactions within the targeting complex vis-à-vis the rates of substrate's escape into the bulk solution at each reaction/relocation step. In this setting, superchanneling may either obtain or not obtain essentially independently of whether or not a targeting complex exhibits an efficacious substrate channeling. The envisioned, and so far hypothetical, processes of substrate channeling and superchanneling are diagrammed in Fig. 7, using notations of transition probabilities for each reaction step in these mutually compatible mechanisms.

For now, we leave aside approaches to measuring the extent of substrate channeling in these settings and consider a way to address the existence and efficacy of superchanneling (Fig. 7B). Molar ratios of enzymes that reside in an Arg/N-degron-targeting complex to their "free" counterparts in the bulk solution are unknown, awaiting measurements of this partitioning in unperturbed *in vivo* settings. Outside of a targeting complex, in the bulk solution, the enzymatic activities of scNTA1 Nt-amidase and scATE1 R-transferase, and the Nt-Arg-binding capability of scUBR1 E3 would be strictly required for a (later) polyubiquitylation of, for example, an initially Nt-Asn-bearing substrate. That is so because scUBR1 E3 would be unable to recognize (bind to) the above substrate in the bulk solution until after a substrate's Nt modifications have run their course and yielded the (conjugated) Nt-Arg residue that can be (non-covalently) captured by scUBR1 (Figs. 1A and 7).

In contrast, the enzymatic activities of Nt-amidase and R-transferase might be dispensable for superchanneling, which can occur only within a targeting complex. Specifically, if superchanneling is efficacious, the Nt-deamidation activity of the complex-bound scNTA1 Nt-amidase would not be strictly required (or may not be required at all) for polyubiquitylation of an (initially) Nt-Asn-bearing substrate. A nearly wild-type level of physical affinity of scNTA1 for Nt-Asn would still be essential, so that a substrate could be (reversibly) captured by the complex-bound Nt-amidase and thereby (possibly) placed spatially close to the complex-bound scUBR1-RAD6 E3-E2 Ub ligase (Figs. 1A and 7). But Nt-deamidation activity of Nt-amidase may be dispensable in this setting, given the logic of superchanneling model (Fig. 7B).

The crystal structure of the *S. cerevisiae* scNTA1 Nt-amidase was determined by Song and colleagues (62), who also characterized the active site of scNTA1. To address the hypothesis of superchanneling, one could replace, using reverse genetics, the scNTA1 gene with its allele that encodes a missense active-site mutant of scNTA1 that is inactive as Nt-amidase but is essentially unchanged in its affinity for Nt-Asn-bearing substrates. Whether an enzymatically inactive scNTA1 mutant that retains affinity for Nt-Asn is a technically realistic proposition remains to be seen. If the Arg/N-degron pathway exhibits superchanneling, yeast cells expressing wild-type levels of mutant scNTA1 (enzymatically inactive but binding, in particular, to Nt-Asn) might continue to polyubiquitylate and degrade an Nt-Asn-bearing substrate despite the absence of Nt-deamidation in these cells. In contrast, *nta1*Δ cells, which lack the entire

scNTA1 protein, would be unable to target and degrade such a substrate, as has been shown previously (61).

Even a partial retention of polyubiquitylation and degradation of an Nt-Asn-bearing substrate in a missense *nta1* mutant that satisfies the above constraints would suggest the existence of superchanneling. Conversely, if an enzymatically inactive scNTA1 protein (that retains the affinity for Nt-Asn) would be unable to support degradation of an Nt-Asn-bearing substrate, it would be evidence for a weak or absent superchanneling of that substrate.

A general notion of superchanneling is as follows. Consider a multienzyme complex that catalyzes modifications of a protein substrate. Some of these modifications are obligatorily sequential, some are not. At least one ("last") enzyme of the complex can modify the substrate independently of other enzymes. However, the last enzyme cannot bind to (i.e., does not have affinity for) the initial substrate, whereas the first, "upstream" enzyme of the multienzyme complex does. In such a setting, the binding of upstream enzyme to the initial substrate may bring the latter into a stereo/catalytically favorable proximity to the last enzyme of the complex, thereby enabling a substrate's modification by the last enzyme. That modification would bypass, either entirely or in part, the intermediate modification steps. Such a bypass (referred to as superchanneling) may be possible within a proximity-enabling targeting complex, but would be impossible with free enzymes in the bulk solution. In the latter case, intermediate modification steps would be essential for a productive binding of the last enzyme to the (properly modified) substrate. We are working to verify the idea of superchanneling and to also determine the extent of substrate channeling in the yeast and human Arg/N-degron pathways.

Concluding Remarks. Three-dimensional structures of Arg/N-degron-targeting complexes are unknown. This information would be essential for a deeper understanding of these multienzyme assemblies. A previous study has shown that scUBR1 and scUFD4 E3s, which bind to each other (65), also bind to the 26S proteasome (76). That evidence, if viewed together with the present results (Fig. 6), suggests an even larger juggernaut of an Arg/N-degron-targeting complex that contains the proteasome as well.

Now that targeting complexes of the Arg/N-degron pathway have been found to exist but remain to be understood, one set of salient questions is about their dynamics and composition. How stable (or fleeting) are these complexes in living cells? How to detect and monitor a "complete" targeting complex *in vivo*? Does assembly of these complexes require chaperones? Do these complexes form constitutively or conditionally, depending on cell's metabolic state? Do they contain other components? [An example of an untested candidate component is *hsLIAT1*, a human protein of unknown function that specifically binds to R-transferase *hsATE1* (108).] It also remains to be determined whether UBR4 (570 kDa) and UBR5 (300 kDa), two other E3 N-recognition proteins of the Arg/N-degron pathway in animals and plants (Fig. 1B) (2, 24, 66–68), function as subunits of multienzyme complexes that are analogous to those containing UBR1 or UBR2.

Materials and Methods

For further information, see *SI Appendix, SI Materials and Methods*.

Yeast Strains and Genetic Techniques. *S. cerevisiae* strains used in this work are described in *SI Appendix, Table S1*. Standard techniques were used for strain construction and transformation.

Construction of Plasmids. The plasmids are described in *SI Appendix, Table S2*. Construction details are described in *SI Appendix, Materials and Methods*.

Two-Hybrid Assays. Y2H assays (87) were carried out as described previously (9, 10, 28, 86). In both Y2H and split-Ub assays, the expression of *HIS3* (a readout of both assays), in otherwise His⁻ cells, was a function of affinity between test proteins.

Split-Ub Assays. Yeast-based split-Ub binding assays (93, 94) were carried out largely as described previously (9, 28).

GST-Pulldowns. These binding assays were carried out with yeast extracts largely as described previously (90), using, in particular, *E. coli*-expressed, purified fusions of human test proteins with GST.

Co-IP Assays. These binding assays were carried out with yeast extracts largely as described previously (90), using engineered *S. cerevisiae* strains that stably coexpressed specific epitope-tagged human test proteins from their integrated cDNAs (*SI Appendix, Materials and Methods*).

Data Availability. All relevant data in the paper are entirely available through both text and figures, in the main text and *SI Appendix*.

ACKNOWLEDGMENTS. We thank current and former members of the A.V. laboratory for their advice and assistance. This work was supported by the NIH Grants 1R01DK039520 and 1R01GM031530 (to A.V.).

1. A. Hershko, A. Ciechanover, A. Varshavsky, Basic Medical Research Award. The ubiquitin system. *Nat. Med.* **6**, 1073–1081 (2000).
2. A. Varshavsky, N-degron and C-degron pathways of protein degradation. *Proc. Natl. Acad. Sci. U.S.A.* **116**, 358–366 (2019).
3. D. Finley, H. D. Ulrich, T. Sommer, P. Kaiser, The ubiquitin-proteasome system of *Saccharomyces cerevisiae*. *Genetics* **192**, 319–360 (2012).
4. V. Vittal, M. D. Stewart, P. S. Brzovic, R. E. Klevit, Regulating the regulators: Recent revelations in the control of E3 ubiquitin ligases. *J. Biol. Chem.* **290**, 21244–21251 (2015).
5. C. Pohl, I. Dikic, Cellular quality control by the ubiquitin-proteasome system and autophagy. *Science* **366**, 818–822 (2019).
6. C. H. Ji, Y. T. Kwon, Crosstalk and interplay between the ubiquitin-proteasome system and autophagy. *Mol. Cells* **40**, 441–449 (2017).
7. D. Balchin, M. Hayer-Hartl, F. U. Hartl, In vivo aspects of protein folding and quality control. *Science* **353**, aac4354 (2016).
8. Z. Sun, J. L. Brodsky, Protein quality control in the secretory pathway. *J. Cell Biol.* **218**, 3171–3187 (2019).
9. J. H. Oh, J. Y. Hyun, A. Varshavsky, Control of Hsp90 chaperone and its clients by N-terminal acetylation and the N-end rule pathway. *Proc. Natl. Acad. Sci. U.S.A.* **114**, E4370–E4379 (2017).
10. S. J. Chen, A. Melnykov, A. Varshavsky, Evolution of substrates and components of the pro/N-degron pathway. *Biochemistry* **59**, 582–593 (2020).
11. N. Zheng, N. Shabek, Ubiquitin ligases: Structure, function, and regulation. *Annu. Rev. Biochem.* **86**, 129–157 (2017).
12. E. R. Watson, N. G. Brown, J. M. Peters, H. Stark, B. A. Schulman, Posing the APC/C E3 ubiquitin ligase to orchestrate cell division. *Trends Cell Biol.* **29**, 117–134 (2019).
13. M. Schapira, M. F. Calabrese, A. N. Bullock, C. M. Crews, Targeted protein degradation: Expanding the toolbox. *Nat. Rev. Drug Discov.* **18**, 949–963 (2019).
14. J. A. M. Bard *et al.*, Structure and function of the 26S proteasome. *Annu. Rev. Biochem.* **87**, 697–724 (2018).
15. A. Schweitzer *et al.*, Structure of the human 26S proteasome at a resolution of 3.9 Å. *Proc. Natl. Acad. Sci. U.S.A.* **113**, 7816–7821 (2016).
16. D. Finley, M. A. Prado, The proteasome and its network: Engineering for adaptability. *Cold Spring Harb. Perspect. Biol.* **12**, a033985 (2020).
17. G. A. Collins, A. L. Goldberg, The logic of the 26S proteasome. *Cell* **169**, 792–806 (2017).
18. L. Budenholzer, C. L. Cheng, Y. Li, M. Hochstrasser, Proteasome structure and assembly. *J. Mol. Biol.* **429**, 3500–3524 (2017).
19. H. Yu, A. Matouschek, Recognition of client proteins by the proteasome. *Annu. Rev. Biophys.* **46**, 149–173 (2017).
20. A. Bachmair, D. Finley, A. Varshavsky, In vivo half-life of a protein is a function of its amino-terminal residue. *Science* **234**, 179–186 (1986).
21. A. Bachmair, A. Varshavsky, The degradation signal in a short-lived protein. *Cell* **56**, 1019–1032 (1989).
22. A. Varshavsky, The N-end rule pathway and regulation by proteolysis. *Protein Sci.* **20**, 1298–1345 (2011).
23. D. A. Dougan, D. Micevski, K. N. Truscott, The N-end rule pathway: From recognition by N-recognins, to destruction by AAA+proteases. *Biochim. Biophys. Acta* **1823**, 83–91 (2012).
24. T. Tasaki, S. M. Sriram, K. S. Park, Y. T. Kwon, The N-end rule pathway. *Annu. Rev. Biochem.* **81**, 261–289 (2012).
25. H. Aksnes, A. Drazic, M. Marie, T. Arnesen, First things first: Vital protein marks by N-terminal acetyltransferases. *Trends Biochem. Sci.* **41**, 746–760 (2016).
26. D. J. Gibbs, J. Bacardit, A. Bachmair, M. J. Holdsworth, The eukaryotic N-end rule pathway: Conserved mechanisms and diverse functions. *Trends Cell Biol.* **24**, 603–611 (2014).
27. N. Dissmeyer, S. Rivas, E. Graciet, Life and death of proteins after protease cleavage: Protein degradation by the N-end rule pathway. *New Phytol.* **218**, 929–935 (2018).
28. S. J. Chen, X. Wu, B. Vadas, J.-H. Oh, A. Varshavsky, An N-end rule pathway that recognizes proline and destroys gluconeogenic enzymes. *Science* **355**, eaal3655 (2017).
29. C. Dong *et al.*, Molecular basis of GID4-mediated recognition of degrons for the pro/N-end rule pathway. *Nat. Chem. Biol.* **14**, 466–473 (2018).
30. D. A. Dougan, A. Varshavsky, Understanding the pro/N-end rule pathway. *Nat. Chem. Biol.* **14**, 415–416 (2018).
31. J. M. Kim *et al.*, Formyl-methionine as an N-degron of a eukaryotic N-end rule pathway. *Science* **362**, eaat0174 (2018).
32. C. S. Hwang, A. Shemorry, A. Varshavsky, N-terminal acetylation of cellular proteins creates specific degradation signals. *Science* **327**, 973–977 (2010).
33. K. I. Piatkov, C. S. Brower, A. Varshavsky, The N-end rule pathway counteracts cell death by destroying proapoptotic protein fragments. *Proc. Natl. Acad. Sci. U.S.A.* **109**, E1839–E1847 (2012).
34. C. S. Brower, K. I. Piatkov, A. Varshavsky, Neurodegeneration-associated protein fragments as short-lived substrates of the N-end rule pathway. *Mol. Cell* **50**, 161–171 (2013).
35. Y. A. T. Kasu, S. Alemu, A. Lamari, N. Loew, C. S. Brower, The N-termini of TAR DNA-binding protein 43 (TDP43) C-terminal fragments influence degradation, aggregation propensity, and morphology. *Mol. Cell Biol.* **38**, e00243-18 (2018).
36. H. K. Kim *et al.*, The N-terminal methionine of cellular proteins as a degradation signal. *Cell* **156**, 158–169 (2014).
37. K. T. Nguyen *et al.*, N-terminal acetylation and the N-end rule pathway control degradation of the lipid droplet protein PLIN2. *J. Biol. Chem.* **294**, 379–388 (2019).
38. A. Shemorry, C. S. Hwang, A. Varshavsky, Control of protein quality and stoichiometries by N-terminal acetylation and the N-end rule pathway. *Mol. Cell* **50**, 540–551 (2013).
39. R. F. Shearer, M. Iconomou, C. K. Watts, D. N. Saunders, Functional roles of the E3 ubiquitin ligase UBR5 in cancer. *Mol. Cancer Res.* **13**, 1523–1532 (2015).
40. I. Rivera-Rivera, G. Román-Hernández, R. T. Sauer, T. A. Baker, Remodeling of a delivery complex allows Clp5-mediated degradation of N-degron substrates. *Proc. Natl. Acad. Sci. U.S.A.* **111**, E3853–E3859 (2014).
41. Y. D. Yoo *et al.*, N-terminal arginylation generates a bimodal degron that modulates autophagic proteolysis. *Proc. Natl. Acad. Sci. U.S.A.* **115**, E2716–E2724 (2018).
42. J. Vicente *et al.*, The Cys-Arg/N-end rule pathway is a general sensor of abiotic stress in flowering plants. *Curr. Biol.* **27**, 3183–3190.e4 (2017).
43. J. H. Oh, S. J. Chen, A. Varshavsky, A reference-based protein degradation assay without global translation inhibitors. *J. Biol. Chem.* **292**, 21457–21465 (2017).
44. N. Masson *et al.*, Conserved N-terminal cysteine dioxygenases transduce responses to hypoxia in animals and plants. *Science* **365**, 65–69 (2019).
45. X. Gao, J. Yeom, E. A. Groisman, The expanded specificity and physiological role of a widespread N-degron recognin. *Proc. Natl. Acad. Sci. U.S.A.* **116**, 18629–18637 (2019).
46. R. T. Timms *et al.*, A glycine-specific N-degron pathway mediates the quality control of protein N-myristoylation. *Science* **365**, eaaw4912 (2019).
47. J. S. Park *et al.*, Structural analyses on the deamidation of N-terminal Asn in the human N-degron pathway. *Biomolecules* **10**, 163 (2020).
48. S. Qiao *et al.*, Interconversion between anticipatory and active GID E3 ubiquitin ligase conformations via metabolically driven substrate receptor assembly. *Mol. Cell* **77**, 150–163.e9 (2020).
49. T. Inobe, S. Fishbain, S. Prakash, A. Matouschek, Defining the geometry of the two-component proteasome degron. *Nat. Chem. Biol.* **7**, 161–167 (2011).
50. Y. T. Kwon *et al.*, Altered activity, social behavior, and spatial memory in mice lacking the NTAN1p amidase and the asparagine branch of the N-end rule pathway. *Mol. Cell Biol.* **20**, 4135–4148 (2000).
51. K. I. Piatkov, J.-H. Oh, Y. Liu, A. Varshavsky, Calpain-generated natural protein fragments as short-lived substrates of the N-end rule pathway. *Proc. Natl. Acad. Sci. U.S.A.* **111**, E817–E826 (2014).
52. M. A. Eldeeb, R. P. Fahlman, The anti-apoptotic form of tyrosine kinase Lyn that is generated by proteolysis is degraded by the N-end rule pathway. *Oncotarget* **5**, 2714–2722 (2014).
53. E. Graciet *et al.*, Aminoacyl-transferases and the N-end rule pathway in a human pathogen. *Proc. Natl. Acad. Sci. U.S.A.* **103**, 3078–3083 (2006).
54. K. I. Piatkov, L. Colnaghi, M. Békés, A. Varshavsky, T. T. Huang, The auto-generated fragment of the Usp1 deubiquitylase is a physiological substrate of the N-end rule pathway. *Mol. Cell* **48**, 926–933 (2012).
55. D. J. Gibbs, M. J. Holdsworth, Every breath you take: New insights into plant and animal oxygen sensing. *Cell* **180**, 22–24 (2020).
56. B. P. Weaver, Y. M. Weaver, S. Mitani, M. Han, Coupled caspase and N-end rule ligase activities allow recognition and degradation of pluripotency factor LIN-28 during non-apoptotic development. *Dev. Cell* **41**, 665–673.e6 (2017).
57. N. B. Nillegoda *et al.*, Ubr1 and Ubr2 function in a quality control pathway for degradation of unfolded cytosolic proteins. *Mol. Biol. Cell* **21**, 2102–2116 (2010).
58. K. Yamano, R. J. Youle, PINK1 is degraded through the N-end rule pathway. *Autophagy* **9**, 1758–1769 (2013).
59. W. S. Choi *et al.*, Structural basis for the recognition of N-end rule substrates by the UBR box of ubiquitin ligases. *Nat. Struct. Mol. Biol.* **17**, 1175–1181 (2010).
60. E. Matta-Camacho, G. Kozlov, F. F. Li, K. Gehring, Structural basis of substrate recognition and specificity in the N-end rule pathway. *Nat. Struct. Mol. Biol.* **17**, 1182–1187 (2010).

61. R. T. Baker, A. Varshavsky, Yeast N-terminal amidase. A new enzyme and component of the N-end rule pathway. *J. Biol. Chem.* **270**, 12065–12074 (1995).
62. M. K. Kim, S. J. Oh, B. G. Lee, H. K. Song, Structural basis for dual specificity of yeast N-terminal amidase in the N-end rule pathway. *Proc. Natl. Acad. Sci. U.S.A.* **113**, 12438–12443 (2016).
63. G. C. Turner, F. Du, A. Varshavsky, Peptides accelerate their uptake by activating a ubiquitin-dependent proteolytic pathway. *Nature* **405**, 579–583 (2000).
64. F. Du, F. Navarro-Garcia, Z. Xia, T. Tasaki, A. Varshavsky, Pairs of dipeptides synergistically activate the binding of substrate by ubiquitin ligase through dissociation of its autoinhibitory domain. *Proc. Natl. Acad. Sci. U.S.A.* **99**, 14110–14115 (2002).
65. C. S. Hwang, A. Shemorry, D. Auerbach, A. Varshavsky, The N-end rule pathway is mediated by a complex of the RING-type Ubr1 and HECT-type Ufd4 ubiquitin ligases. *Nat. Cell Biol.* **12**, 1177–1185 (2010).
66. S. T. Kim *et al.*, The N-recogin UBR4 of the N-end rule pathway is required for neurogenesis and homeostasis of cell surface proteins. *PLoS One* **13**, e0202260 (2018).
67. M. M. Rinschen *et al.*, The ubiquitin ligase Ubr4 controls stability of podocin/MEC-2 supercomplexes. *Hum. Mol. Genet.* **25**, 1328–1344 (2016).
68. J. E. Flack, J. Mieszczanek, N. Novic, M. Bienz, Wnt-dependent inactivation of the Groucho/TLE co-repressor by the HECT E3 ubiquitin ligase Hyd/UBR5. *Mol. Cell* **67**, 181–193.e5 (2017).
69. H. Cha-Molstad *et al.*, Regulation of autophagic proteolysis by the N-recogin SQSTM1/p62 of the N-end rule pathway. *Autophagy* **14**, 359–361 (2018).
70. D. H. Kwon *et al.*, Insights into degradation mechanism of N-end rule substrates by p62/SQSTM1 autophagy adapter. *Nat. Commun.* **9**, 3291 (2018).
71. A. Varshavsky, “Spalog” and “sequelog”: Neutral terms for spatial and sequence similarity. *Curr. Biol.* **14**, R181–R183 (2004).
72. H. Wang, K. I. Piatkov, C. S. Brower, A. Varshavsky, Glutamine-specific N-terminal amidase, a component of the N-end rule pathway. *Mol. Cell* **34**, 686–695 (2009).
73. R.-G. Hu *et al.*, The N-end rule pathway as a nitric oxide sensor controlling the levels of multiple regulators. *Nature* **437**, 981–986 (2005).
74. M. J. Lee *et al.*, RG54 and RG55 are in vivo substrates of the N-end rule pathway. *Proc. Natl. Acad. Sci. U.S.A.* **102**, 15030–15035 (2005).
75. M. S. Park *et al.*, Crystal structure of human protein N-terminal glutamine amidohydrolase, an initial component of the N-end rule pathway. *PLoS One* **9**, e111142 (2014).
76. Y. Xie, A. Varshavsky, Physical association of ubiquitin ligases and the 26S proteasome. *Proc. Natl. Acad. Sci. U.S.A.* **97**, 2497–2502 (2000).
77. I. Wheeldon *et al.*, Substrate channelling as an approach to cascade reactions. *Nat. Chem.* **8**, 299–309 (2016).
78. F. M. Raushel, J. B. Thoden, H. M. Holden, Enzymes with molecular tunnels. *Acc. Chem. Res.* **36**, 539–548 (2003).
79. G. R. Welch, J. S. Easterby, Metabolic channeling versus free diffusion: Transition-time analysis. *Trends Biochem. Sci.* **19**, 193–197 (1994).
80. N. Sathyanarayanan *et al.*, Molecular basis for metabolite channeling in a ring opening enzyme of the phenylacetate degradation pathway. *Nat. Commun.* **10**, 4127 (2019).
81. M. Castellana *et al.*, Enzyme clustering accelerates processing of intermediates through metabolic channeling. *Nat. Biotechnol.* **32**, 1011–1018 (2014).
82. X. Zhao *et al.*, Substrate-driven chemotactic assembly in an enzyme cascade. *Nat. Chem.* **10**, 311–317 (2018).
83. M. F. Dunn, D. Niks, H. Ngo, T. R. Barends, I. Schlichting, Tryptophan synthase: The workings of a channeling nanomachine. *Trends Biochem. Sci.* **33**, 254–264 (2008).
84. H. Lee, W. C. DeLoache, J. E. Dueber, Spatial organization of enzymes for metabolic engineering. *Metab. Eng.* **14**, 242–251 (2012).
85. A. M. Pedley, S. J. Benkovic, A New view into the regulation of purine metabolism: The purinosome. *Trends Biochem. Sci.* **42**, 141–154 (2017).
86. A. Melnykov, S. J. Chen, A. Varshavsky, Gid10 as an alternative N-recogin of the pro/N-degron pathway. *Proc. Natl. Acad. Sci. U.S.A.* **116**, 15914–15923 (2019).
87. M. Vidal, S. Fields, The yeast two-hybrid assay: Still finding connections after 25 years. *Nat. Methods* **11**, 1203–1206 (2014).
88. A. Brückner, C. Polge, N. Lentze, D. Auerbach, U. Schlattner, Yeast two-hybrid, a powerful tool for systems biology. *Int. J. Mol. Sci.* **10**, 2763–2788 (2009).
89. T. Stellberger *et al.*, Improving the yeast two-hybrid system with permuted fusions proteins: The Varicella Zoster virus interactome. *Proteome Sci.* **8**, 8 (2010).
90. F. M. Ausubel, Ed. *et al.*, *Current Protocols in Molecular Biology*, (Wiley-Interscience, New York, 2017).
91. Y. T. Kwon *et al.*, An essential role of N-terminal arginylation in cardiovascular development. *Science* **297**, 96–99 (2002).
92. Y. T. Kwon, A. S. Kashina, A. Varshavsky, Alternative splicing results in differential expression, activity, and localization of the two forms of arginyl-tRNA-protein transferase, a component of the N-end rule pathway. *Mol. Cell. Biol.* **19**, 182–193 (1999).
93. N. Johnsson, A. Varshavsky, Split ubiquitin as a sensor of protein interactions in vivo. *Proc. Natl. Acad. Sci. U.S.A.* **91**, 10340–10344 (1994).
94. A. Dünkler, J. Müller, N. Johnsson, Detecting protein-protein interactions with the split-Ubiquitin sensor. *Methods Mol. Biol.* **786**, 115–130 (2012).
95. Z. Xia, G. C. Turner, C. S. Hwang, C. Byrd, A. Varshavsky, Amino acids induce peptide uptake via accelerated degradation of CUP9, the transcriptional repressor of the PTR2 peptide transporter. *J. Biol. Chem.* **283**, 28958–28968 (2008).
96. T. Gudjonsson *et al.*, TRIP12 and UBR5 suppress spreading of chromatin ubiquitylation at damaged chromosomes. *Cell* **150**, 697–709 (2012).
97. Y. Park, S. K. Yoon, J. B. Yoon, The HECT domain of TRIP12 ubiquitinates substrates of the ubiquitin fusion degradation pathway. *J. Biol. Chem.* **284**, 1540–1549 (2009).
98. X. Liu *et al.*, Trip12 is an E3 ubiquitin ligase for USP7/HAUSP involved in the DNA damage response. *FEBS Lett.* **590**, 4213–4222 (2016).
99. N. Hanoun *et al.*, The E3 ubiquitin ligase thyroid hormone receptor-interacting protein 12 targets pancreas transcription factor 1a for proteasomal degradation. *J. Biol. Chem.* **289**, 35593–35604 (2014).
100. M. J. Holdsworth, J. Vicente, G. Sharma, M. Abbas, A. Zubrycka, The plant N-degron pathways of ubiquitin-mediated proteolysis. *J. Integr. Plant Biol.* **62**, 70–89 (2020).
101. D. A. Weits *et al.*, Plant cysteine oxidases control the oxygen-dependent branch of the N-end-rule pathway. *Nat. Commun.* **5**, 3425 (2014).
102. A. Ciechanover *et al.*, Purification and characterization of arginyl-tRNA-protein transferase from rabbit reticulocytes. Its involvement in post-translational modification and degradation of acidic NH₂ termini substrates of the ubiquitin pathway. *J. Biol. Chem.* **263**, 11155–11167 (1988).
103. R. J. Dohmen, K. Madura, B. Bartel, A. Varshavsky, The N-end rule is mediated by the UBC2(RAD6) ubiquitin-conjugating enzyme. *Proc. Natl. Acad. Sci. U.S.A.* **88**, 7351–7355 (1991).
104. A. Varshavsky, The N-end rule: Functions, mysteries, uses. *Proc. Natl. Acad. Sci. U.S.A.* **93**, 12142–12149 (1996).
105. B. Bartel, I. Wüning, A. Varshavsky, The recognition component of the N-end rule pathway. *EMBO J.* **9**, 3179–3189 (1990).
106. F. Du, “Allosteric activation of the ubiquitin ligase UBR1 by short peptides: Molecular mechanisms and physiological functions,” PhD thesis, California Institute of Technology, Pasadena, CA (2001).
107. S. Albert *et al.*, Direct visualization of degradation microcompartments at the ER membrane. *Proc. Natl. Acad. Sci. U.S.A.* **117**, 1069–1080 (2020).
108. C. S. Brower *et al.*, Liat1, an arginyltransferase-binding protein whose evolution among primates involved changes in the numbers of its 10-residue repeats. *Proc. Natl. Acad. Sci. U.S.A.* **111**, E4936–E4945 (2014).
109. Y. Xie, A. Varshavsky, The E2-E3 interaction in the N-end rule pathway: The RING-H2 finger of E3 is required for the synthesis of multiubiquitin chain. *EMBO J.* **18**, 6832–6844 (1999).
110. D. K. Worthyake, S. Prakash, L. Prakash, C. P. Hill, Crystal structure of the *Saccharomyces cerevisiae* ubiquitin-conjugating enzyme Rad6 at 2.6 Å resolution. *J. Biol. Chem.* **273**, 6271–6276 (1998).
111. W. J. Cook, L. C. Jeffrey, Y. Xu, V. Chau, Tertiary structures of class I ubiquitin-conjugating enzymes are highly conserved: Crystal structure of yeast Ubc4. *Biochemistry* **32**, 13809–13817 (1993).